Characterization of Plasma-sprayed Zirconia Coatings by X-ray Diffraction and Raman Spectroscopy†

Nobuya IWAMOTO*, Norimasa UMESAKI** and Shigeki ENDO***

Abstract

Three zirconia ceramics, ZrO_2-4.5mol%Y_2O_3, ZrO_2-12mol%Y_2O_3, and ZrO_2-8mol%MgO, before and after plasma spraying were investigated by X-ray diffraction. The amounts of monoclinic, tetragonal and cubic phases existing in the three zirconia ceramics were determined from the integrated intensity ratios in the {400} and {111} regions of the X-ray diffraction patterns. Tetragonal-to-monoclinic transformation in the plasma-sprayed coatings caused by indentation, fracture and/or heat treatment of laser beam was examined by Raman spectroscopy. As a result, this spectroscopic technique is shown to be a powerful tool for the observation of this transformation. Furthermore, microanalysis of the coatings was performed by the use of Raman microprobe spectroscopy.

KEY WORDS: (Plasma Spraying) (Zirconia Coating) (X-ray Diffraction) (Raman Spectroscopy)

1. Introduction

Numerous plasma-sprayed zirconia-based ceramic coatings with Y_2O_3, MgO, CaO, etc. are widely used as thermal barrier coatings for gas turbine and other heat engine components[1-3]. These coatings reduce the surface temperature of the metal components and act as a barrier to the hot-corrosion degradation of the substrates.

There are three well-defined polymorphs; monoclinic, tetragonal and cubic phases, in ZrO_2-based ceramics less than 12mol% (see the reported ZrO_2-Y_2O_3 phase diagrams[4-6]). Consequently, the ZrO_2-based coatings prepared by plasma spraying are formed from any of the three phases. It is well known that an irreversible transformation from the tetragonal to monoclinic phase[7] is caused by mechanical impacts such as fracture, indentation, heating and thermal cycles, etc., and remarkably effects the various properties of the coatings. Therefore, it is important to examine the tetragonal-to-monoclinic transformation occurring in the coatings during various mechanical impacts. Phillippi et al.[8] determined the Raman active bands of the three phases in zirconia crystals. Keramidas et al.[9] indicated that X-ray and electron diffraction analyses are insensitive to such structural change of intermediate-range order, while Raman spectroscopy is sensitive to it. Benner et al.[10] examined the transformation behavior of Y_2O_3-stabilized ZrO_2 coatings, which are prepared by physical vapor deposition on an IN-738 substrate with an Ni-Cr-Al-Y under coating, by means of high temperature Raman spectroscopy up to 1050°C. According to their investigation, the crystal phase of ZrO_2-8wt.%Y_2O_3 coating is tetragonal, while the ZrO_2-12wt.%Y_2O_3 coating consists of cubic phase with a small quantity of tetragonal phase. Marshall[11] reported the application of indentation fracture analysis in ceramics to Vickers indentation. Recently, Clarke et al.[12] studied the transformation-zone sizes of sintered zirconia ceramics during Vickers indentation fracture by Raman microprobe spectroscopy. Up to now, however, the useful Raman technique has not been applied to the plasma-sprayed zirconia coatings.

Therefore, the purpose of this investigation is to analyze the tetragonal-to-monoclinic transformation of three plasma-sprayed coatings, ZrO_2-4.5mol%(8wt.%)-Y_2O_3, ZrO_2-12mol%(20wt.%)Y_2O_3 and ZrO_2-8mol%(2.77 wt.%)MgO, caused by Vickers indentation, fracture and/or heat treatment of laser beam. In addition, monoclinic, tetragonal and cubic phases existing in the three zirconia ceramics before and after plasma spraying were examined by X-ray diffraction. Furthermore, transformation zone size of the ZrO_2-4.5mol%Y_2O_3 coating caused by Vickers indentation is determined using Raman microprobe spectroscopy.

† Received on April 30, 1985
* Professor
** Research Instructor
*** Graduate Student

Transactions of JWRI is published by Welding Research Institute of Osaka University, Ibaraki, Osaka 567, Japan

2. Experimental

Three commercially prepared zirconia ceramic powders, ZrO_2-4.5mol%Y_2O_3 (particle size: 10 ~ 44 μm)$^+$, ZrO_2-12mol%Y_2O_3 (10 ~ 87 μm)$^{++}$ and ZrO_2-8mol%MgO (10 ~ 44 μm)$^+$ were used for plasma spraying, and SUS 316 stainless steel plates (size: 100x25x3 mm) were used as substrate metals. One side of the surface of each steel plate was blasted by Al_2O_3 sand before plasma spraying, and the average surface roughness of the sand blasted substrates was 2.7 μm. The three zirconia ceramic coatings were made with the following plasma spraying conditions;

Plasma spraying equipment: METCO 7M type,
Voltage and Current: 65-70 V and 500 A,
Arc gases: Primary, Ar (40 l/min in 0.65 MPa),
Secondary, H_2 (7.5 l/min in 0.35 MPa),
Powder feed rate: 90 g/min,
Powder carrier gas: Ar (37 l/min),
Spraying distance: 100 mm,
Cooling of substrate: Air blowing,
Thickness of coating: 300 μm.

Other conditions were selected according to METCO technical bulletin. After plasma spraying, the coatings were ground until flat surface ($R_a \leqslant 1$ μm) were produced. Then 20 kg Vickers hardness indentations were made in the surfaces to produce five well-defined indentations per 1 mm^2. The crack formed by Vickers indentation was a square with a side about 240 μm long. On the other hand, a heat treatment of ZrO_2-12mol%Y_2O_3 coating was carried out by a CO_2 gas laser beam; laser power: 2 kW, beam size: 5 mmϕ, and scanning speed: 100 mm/s. The average thickness of the heat-treated zone was about 120 μm.

X-ray diffraction experiment for the three zirconia ceramic coatings was performed with the use of a θ-θ diffractometer with parafocusing geometry and CuK_α (40 kV and 20 mA) radiation monochromatized by a curved graphite monochromator mounted in the diffraction beam. A scanning speed was 1°/min. Especially, in order to make the quantitative analysis of monoclinic, tetragonal and cubic phases existing in the three coatings, the step-scanning technique at $\Delta 2\theta = 0.02°$ intervals was used in the two regions from $2\theta = 27.5°$ to 32.0° for (111) of the tetragonal and cubic phases and (111) and (111) of the monoclinic phase, and from $2\theta = 72.5°$ to 76.0° for (400) of the cubic phase and (004) and (400) of the tetragonal phase; 2θ is the scattering angle. Over the whole range of scattering angle using step-scanning, X-ray intensity per datum point was accumulated for the period of 10~40 s.

Raman spectra were measured on a JASCO model R-800 double-grating spectrometer at a scattering angle of 90°. The Raman scattering geometry is shown in **Fig. 1**. The excitation source was 4880 Å (20492 cm^{-1}) line of NEC GLG-3300 Ar^+ ion laser at power from 300 to 500 mW. The beam diameter was about 1 mmϕ. A set of measurements was repeated four times to determine the reproducibility of the intensity measurements. Furthermore, microanalysis of the ZrO_2-4.5mol%Y_2O_3 coating was performed by the use of JASCO model R-MPS-01 Raman microprobe, as shown in **Fig. 2**.

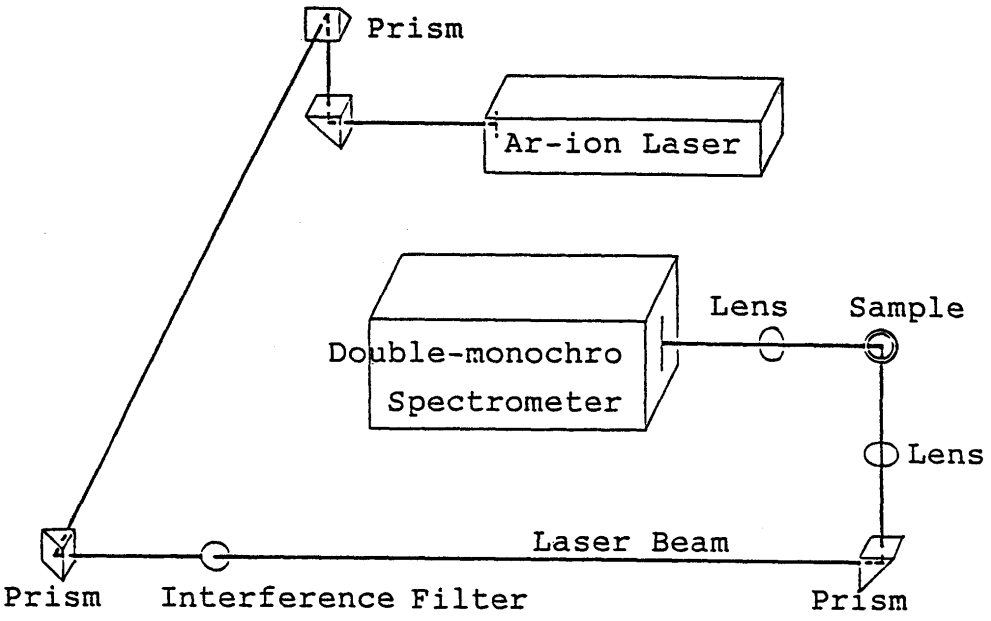

Fig. 1 Optical system of Raman spectroscopy.

$^+$ Shouwa Denko Co., Ltd., Japan (preparation of powder: electrical melting and then pulverizing)
$^{++}$ METCO 202NS (preparation of powder: blending)

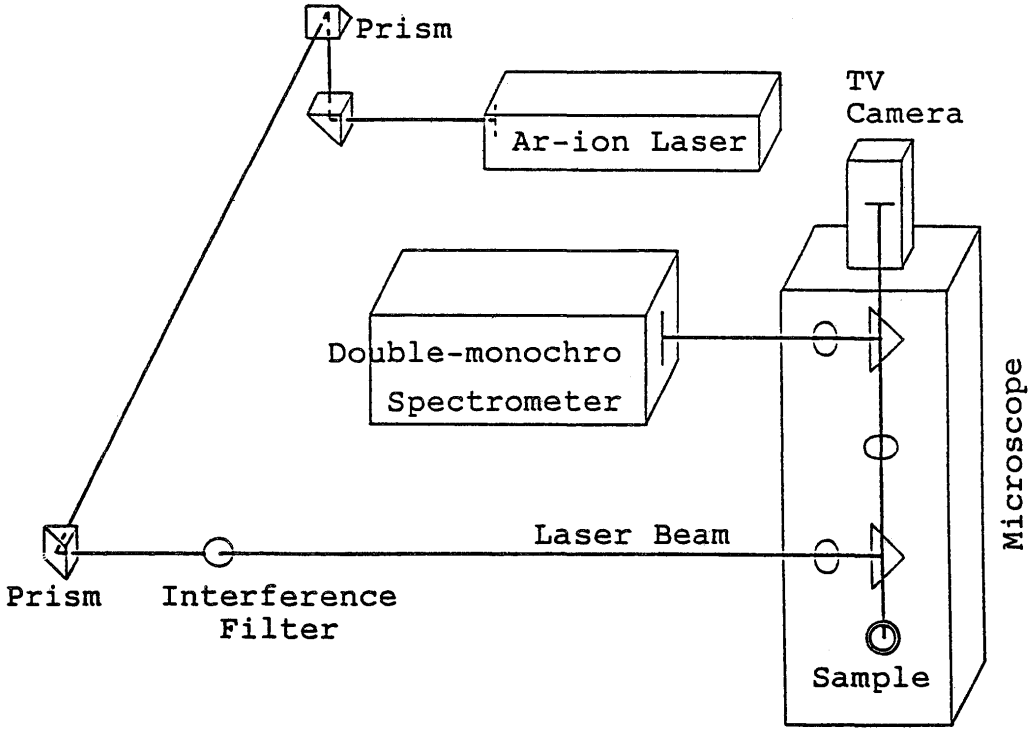

Fig. 2 Optical system of Raman microprobe.

3. Results and Discussion

3.1 X-ray diffraction

X-ray measurement gave the following results. ZrO_2-4.5mol%Y_2O_3 and ZrO_2-8mol%MgO before and after spraying were mixtures of monoclinic and stabilized zirconia, and ZrO_2-12mol%Y_2O_3 was a mixture of monoclinic zirconia and Y_2O_3. After spraying, most of them became and stabilized zirconia.

Integrated X-ray intensity ratios obtained for monoclinic, tetragonal and cubic phases can be converted to approximate mole ratios using the following equations (1) ~ (3)[13].

$$C_m = \frac{0.82[I_m(11\bar{1}) + I_m(111)]}{0.82[I_m(11\bar{1}) + I_m(111)] + I_{t,c}(111)} \quad (1)$$

$$C_t = (1 - C_m) \times \frac{1.14[I_t(400) + I_t(004)]}{1.14[I_t(400) + I_t(004)] + I_c(400)} \quad (2)$$

$$C_c = 1 - (C_m + C_t) \quad (3)$$

where C_m, C_t and C_c are the mole fractions of monoclinic, tetragonal and cubic phases, respectively. For example, **Figs. 3** and **4** show the X-ray step-scanning patterns used in order to determine the mole fractions of the three phases. **Table 1** gives the mole fractions C_m, C_t and C_c calculated in this way. It is well known that at low Y_2O_3 content (less than 3mol%Y_2O_3) a monoclinic phase is predominantly in ZrO_2-Y_2O_3 system, and with increasing Y_2O_3 content a tetragonal phase predominates, and further increasing of the Y_2O_3 content leads to a cubic phase (see the reported ZrO_2-Y_2O_3 phase diagrams[4-6]). The results obtained for the as-sprayed coatings, ZrO_2-4.5mol%Y_2O_3 and ZrO_2-12mol%Y_2O_3, are in good agreement with the fact described above. As given in Table 1, there are 4% of monoclinic phase, 45% of tetragonal phase and 51% of cubic phase in the sprayed ZrO_2-4.5mol%Y_2O_3 coating. The amounts of tetragonal and monoclinic phases are consistent with this binary phase diagram[5]. It is found that a small amount of monoclinic phase also exists. Miller et al.[13] pointed out that its presence results from the plasma spraying process or from composition inhomogeneities of the starting powder. As shown in Table 1, the starting powders, ZrO_2-4.5mol%Y_2O_3 and ZrO_2-12mol%Y_2O_3, include 36% and 100% of monoclinic phases, respectively. The reason why the ZrO_2-12mol%Y_2O_3 powder retained more monoclinic phase after spraying then the ZrO_2-4.5mol%Y_2O_3 powder is probably that the former powder is not stabilized at all. In the case of ZrO_2-8mol%MgO coating, the amounts obtained for the three phases are also consistent with the ZrO_2-MgO phase diagram[14].

3.2 Raman spectroscopy

Figs. 5, **6** and **7** show the Raman spectra of ZrO_2-4.5mol%Y_2O_3, ZrO_2-12mol%Y_2O_3 and ZrO_2-8mol%MgO before and after plasma spraying, respectively. The Raman

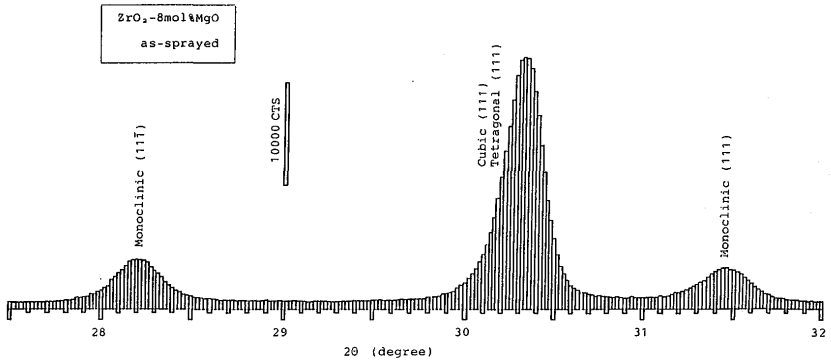

Fig. 3 X-ray step-scanning pattern of plasma-sprayed ZrO_2-8mol% MgO coating for the scanning angle with $2\theta = 27.5°$ to 32.0°.

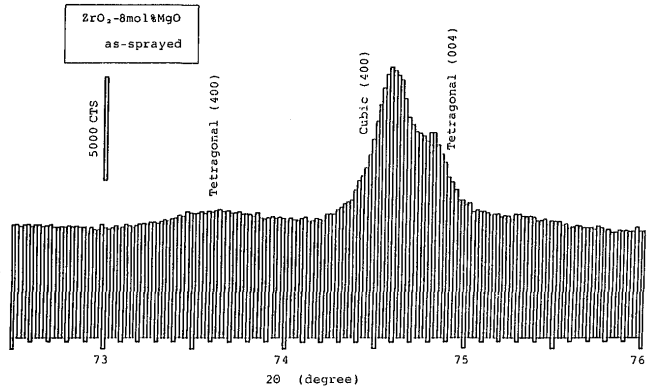

Fig. 4 X-ray step-scanning pattern of plasma-sprayed ZrO_2-8mol% MgO coating for the scanning angle with $2\theta = 72.5°$ to 76.0°.

Table 1 Phase analysis of plasma sprayed zirconia by X-ray diffraction method.

sample		mole ratio		
		C_m	C_t	C_c
ZrO_2-8Y_2O_3	powder	0.36	0.36	0.28
ZrO_2-8Y_2O_3	as-sprayed	0.04	0.45	0.51
ZrO_2-20Y_2O_3	powder*	1.00	0	0
ZrO_2-20Y_2O_3	as-sprayed	0.05	0.22	0.73
ZrO_2-2.77MgO	powder	0.55	0.14	0.31
ZrO_2-2.77MgO	as-sprayed	0.23	0.25	0.52

* this powder also includes Y_2O_3.

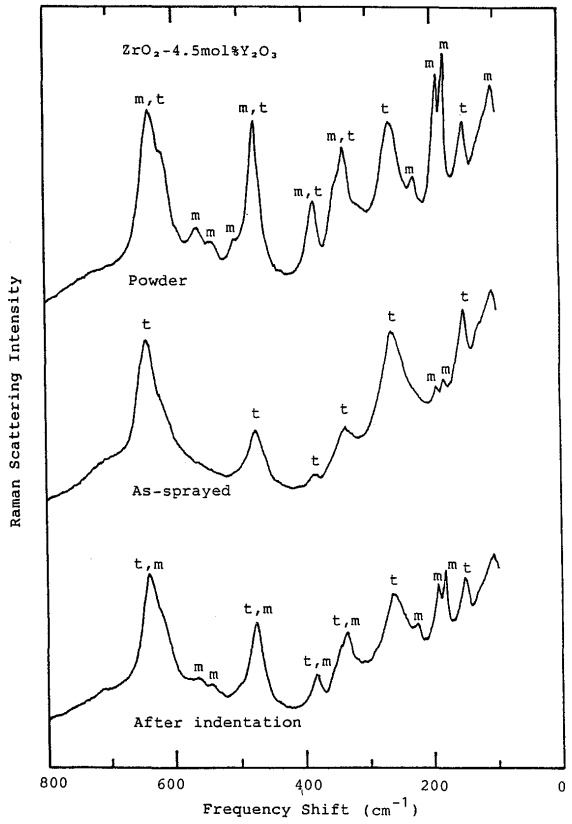

Fig. 5 Raman spectra of ZrO_2-4.5mol%Y_2O_3 before and after plasma spraying and after indenting. m and t are monoclinic and tetragonal phases, respectively.

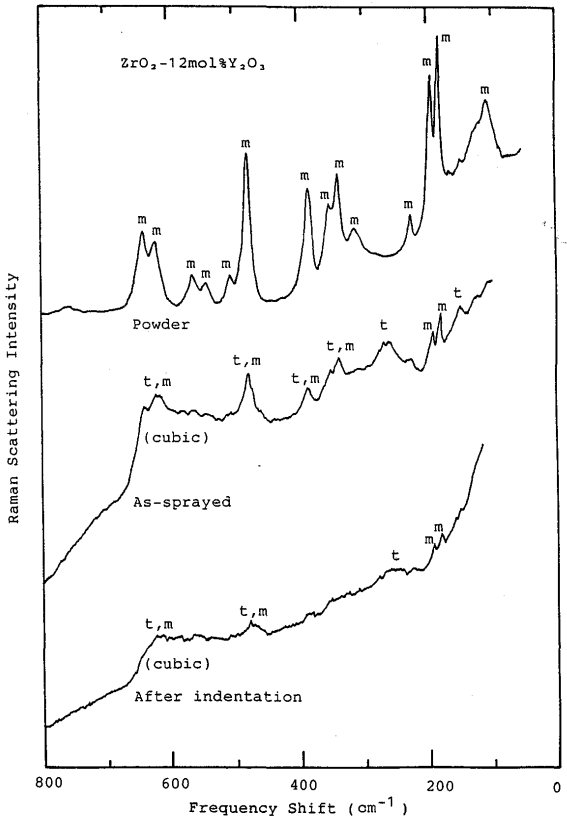

Fig. 6 Raman spectra of ZrO_2-12mol%Y_2O_3 before and after plasma spraying and after indenting.

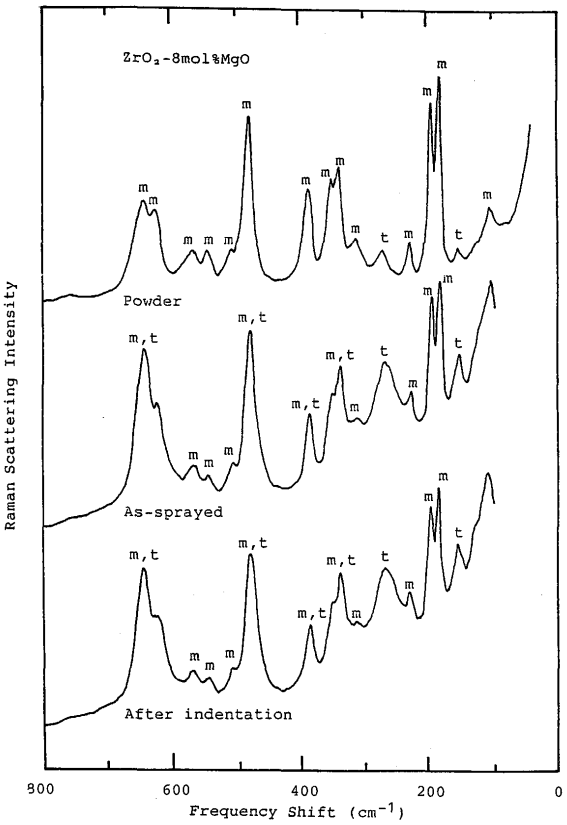

Fig. 7 Raman spectra of ZrO_2-8mol%MgO before and after plasma spraying and after indenting.

bands obtained from the monoclinic, tetragonal and cubic phases are in good agreement with the previous Raman spectroscopic analyses of sintered zirconia ceramics[8,9]. As can be seen in these figures, the Raman bands are especially sensitive to the monoclinic and tetragonal phases. There is some overlap of the monoclinic and tetragonal Raman bands for frequency shifts 300 cm^{-1}, but over the range from 100 cm^{-1} to 300 cm^{-1} these bands are well separated (monoclinic bands: 181 cm^{-1} and 192 cm^{-1}, tetragonal bands: 148 cm^{-1} and 264 cm^{-1}). It is well known that an irreversible transformation from the tetragonal to monoclinic phase is caused by the mechanical impacts already described. Thus we can use these Raman bands for the determination between monoclinic and tetragonal phases. As shown in Fig. 5, a transformation from the tetragonal to monoclinic phases was clearly observed after Vickers indenting. A Raman spectrum from the fractured surface of the ZrO_2-8mol%MgO coating, as can be seen in **Fig. 8**, indicates more drastic transformation than after indenting.

Since the intensity of a Raman band is directly proportional to the concentration of scattering species, we can apply to the determination of the fractions of the monoclinic and tetragonal phases during transformation. Clarke et al.[12] pointed out that the monoclinic and tetragonal concentrations, C_m and C_t, can be expressed directly

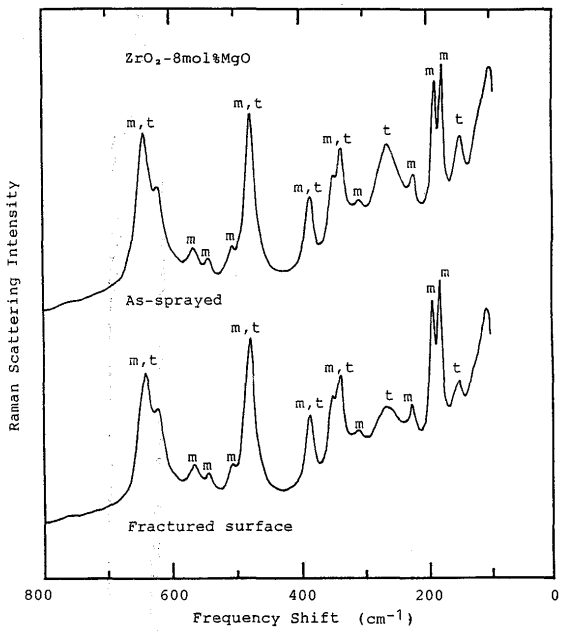

Fig. 8 Raman spectra of ZrO_2-8mol%MgO coating before and after fracture.

in terms of the Raman intensities using the following equation;

$$R(t/t+m) = \frac{T[I^{148} + I^{264}]}{T[I^{148} + I^{264}] + [I^{181} + I^{192}]} \quad (4)$$

where T is the factor to convert the Raman intensities to the concentrations obtained by X-ray diffraction measurement[+++]. The results are given in **Table 2**. The indenting has small effect on the ZrO_2-4.5mol%Y_2O_2 and ZrO_2-8mol%MgO coatings, while it introduces a pronounced transformation for the ZrO_2-4.5mol%Y_2O_3 coating. Up to now, it has been explained that this tetragonal-to-monoclinic transformation is related to the size distribution of zirconia grains, that is, a narrow grain-size distribution leads to a well-defined transformation zone, and a wide grain-size distribution results in a more diffuse transformation zone[7]. It can, therefore, be presumed that the average grain-size of crystalline phases existing in the ZrO_2-4.5mol%Y_2O_3 coating is smaller than that existing

Table 2 Phase analysis of plasma-sprayed Zirconia by Raman spectroscopy.

sample		$R(^t/_{t+m})$	mole ratio	
			C_m	C_t
ZrO_2-4.5mol%Y_2O_3	powder	0.48	0.37	0.35
ZrO_2-4.5mol%Y_2O_3	as-sprayed	0.92	0.04	0.45
ZrO_2-4.5mol%Y_2O_3	after indentation	0.61	0.19	0.30
ZrO_2-12mol%Y_2O_3	powder *	——	1.00	0
ZrO_2-12mol%Y_2O_3	as-sprayed	0.83	0.05	0.22
ZrO_2-12mol%Y_2O_3	after indentation	0.78	0.06	0.21
ZrO_2-8mol%MgO	powder	0.20	0.55	0.14
ZrO_2-8mol%MgO	as-sprayed	0.53	0.23	0.25
ZrO_2-8mol%MgO	after indentation	0.53	0.23	0.25
ZrO_2-8mol%MgO	fractured surface	0.35	0.31	0.17

* this powder also includes Y_2O_3.

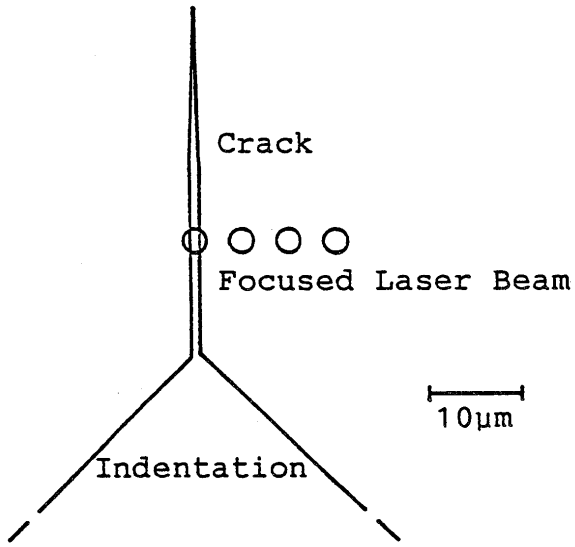

Fig. 9 Schematic diagram illustrating the manner in which the transformation region adjacent to an indentation crack was probed using laser-Raman microprobe.

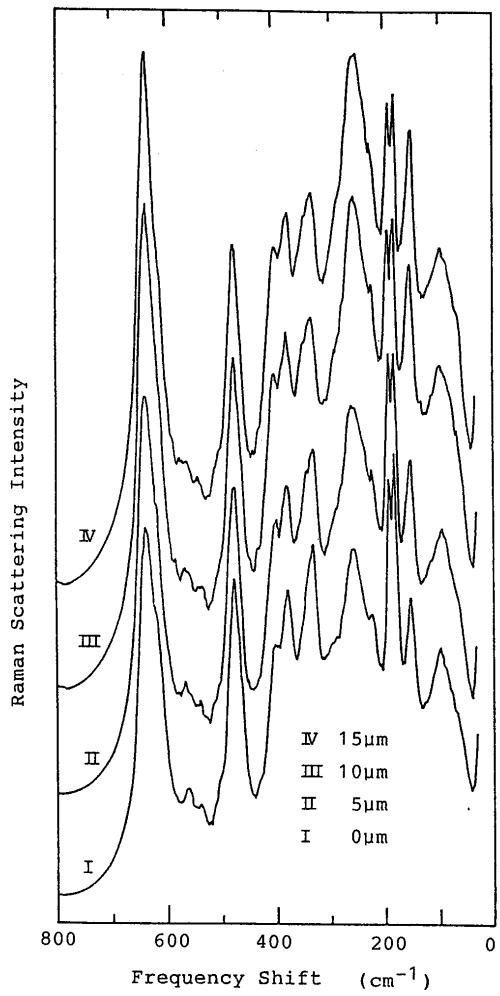

Fig. 10 Raman spectra as a function of distance from an indentation crack in ZrO_2-4.5mol%Y_2O_3 coating.

in the ZrO_2-12mol%Y_2O_3 and/or ZrO_2-8mol%MgO coating.

The Raman spectra obtained at successive distances from a crack in the ZrO_2-4.5mol%Y_2O_3 coating (measured in the geometry of **Fig. 9**) were shown in **Fig. 10**. A nominal probe diameter of 2.5 $\mu m\phi$ was used in collecting the spectra. **Fig. 11** shows the calculated monoclinic/tetragonal concentration as a function of distance from the crack. As shown by Fig. 11, the Raman microprobe indicated that the tetragonal-to-monoclinic transformation zone size was about 12 μm from the crack.

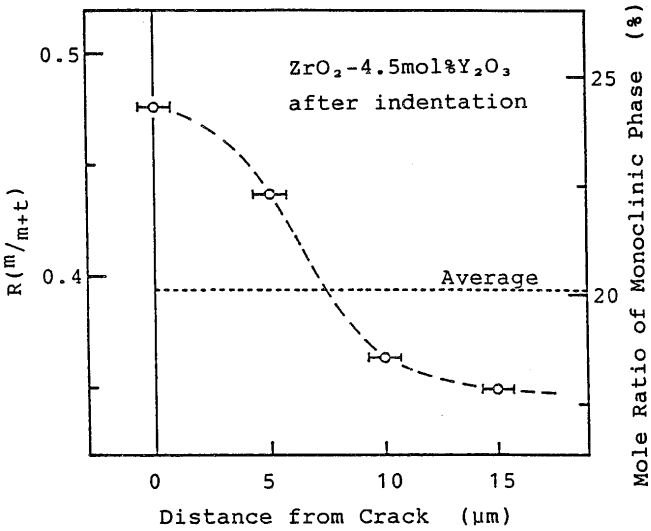

Fig. 11 Concentration of monoclinic phase (m/[m+t] ratio) as a function of distance from an indentation crack in ZrO_2-4.5mol%Y_2O_3 coating determined from Raman microprobe.

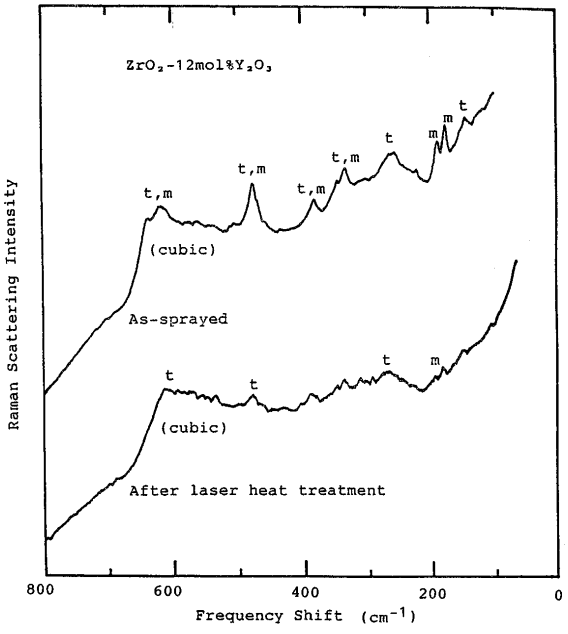

Fig. 12 Raman spectra of ZrO_2-12mol%Y_2O_3 coating before and after laser heart treatment.

+++ Factor T was calculated from both the concentrations of phases determined by X-ray diffraction and the intensities of Raman bands I^{148}, I^{264}, I^{181} and I^{192}. Consequently, it was found to have a remarkable correlation between the concentrations of phases obtained from X-ray diffraction and Raman spectroscopy.

Fig. 12 shows the Raman spectra of the ZrO_2-12mol% Y_2O_3 coating before and after a heat treatment of laser beam. As shown in this figure, the monoclinic phase was greatly decreased by this treatment. This indicates that the surface of the zirconia coating was completely re-melted by laser beam and then was solidified, and results in the formation of more stabilized cubic zirconia. Liu et al.[15] reported the laser surface fusion of M(Ni or Fe)-Cr-Al-Y coatings, but unfortunately the laser treatment of plasma-sprayed ceramic coatings was not studied until now.

4. Conclusion

Three zirconia ceramics, ZrO_2-4.5mol%Y_2O_3, ZrO_2-12mol%Y_2O_3 and ZrO_2-8mol%MgO, before and after plasma spraying were examined by X-ray diffraction. The amounts of monoclinic, tetragonal and cubic phases existing in these samples were determined from the integrated intensity ratios in the {400} and {111} regions of the X-ray diffraction patterns obtained by step-scanning measurement. As a result, it is indicated that most of the three zirconia coatings were stabilized by plasma spraying.

Raman spectra of the three zirconia ceramics before and after plasma spraying were measured, and the obtained data were in good agreement with the previous Raman measurements for sintered zirconia ceramics. Since these Raman spectra were especially sensitive to the monoclinic and tetragonal phases, Raman spectroscopy was applied to the determination of tetragonal-to-monoclinic transformation in the three coatings caused by indentation, fracture and/or heat treatment of laser beam. The results demonstrated that Raman spectroscopy was a powerful technique for determining the transformation in these zirconia coatings. Furthermore, the transformation zone size of the ZrO_2-4.5mol%Y_2O_3 caused by Vickers indentation was determined by the use of Raman microprobe.

Acknowledgement

The authors thank T. Ikeda and M. Yumoto (Nihon Bunko Co., Ltd.) for the Raman microprobe measurement.

References

1) FPRI AP-1539, Part 2, Project 421-1, Final Report, Ceramic Turbine Components Research and Development, August 1980.
2) B.J. Bratton, S.K. Lau and S.Y. Lee, Thin Solid Films, **73** (1980) p.429.
3) A.S. Grot and J.K. Martyn, Am. Ceram. Soc. Bull., **60** (1981) p.807.
4) V.S. Stubican and S.P. Roy, J. Am. Ceram. Soc., **51** (1968) p.38.
5) H.G. Scott, J. Mate, Sci., **10** (1975) p.1527.
6) V.S. Stubican, R.C. Hink and S.P. Roy, J. Am. Ceram. Soc., **61** (1978) p.17.
7) E.C. Subbarao, Advances in Ceramics, Vol.3, in A.H. Heuer and L.W. Hobbs (ed.), Science and Technology of Zirconia, Am. Ceram. Soc., Columbus, Ohio, 1981, p.1.
8) C.M. Phillippi and K.S. Mazdiyasni, J.Am. Ceram. Soc., **54** (1971) p.254.
9) V.G. Keramidas and W.B. White, J. Am. Ceram. Soc., **57** (1974) p.22.
10) R.E. Benner and A.S. Nagelberg, Thin Solid Films, **84** (1981) p.89.
11) D.B. Marshall, J. Am. Ceram. Soc., **66** (1983) p.127.
12) D.R. Clarke and F. Adar, J. Am. Ceram. Soc., **65** (1982) p.284.
13) R.A. Miller, J.L. Smialek and R.G. Garlick, Advances in Ceramics, Vol.3, in A.H. Heuer and L.W. Hobbs (ed.), Science and Technology of Zirconia, Am. Ceram. Soc., Columbus, Ohio, 1981, p.241.
14) C.F. Grain, J. Am. Ceram. Soc., **50** (1967) p.288.
15) C.A. Liu, M.J. Humphries and R.C. Krutenat, Thin Solid Films, **107** (1983) p.269.